

# **Surface Waves and Scattering and Attenuation**

Kiyoshi Yomogida  
Professor  
Graduate School of Science  
Hokkaido University

# CONTENTS

<b>Part I. Surface Waves .....</b>	<b>1</b>
1.1 Love and Rayleigh Waves .....	1
1.2 Dispersion of Surface Waves .....	5
1.3 Measurement of Phase and Group Velocities .....	10
1.4 Estimation of Velocity Structure from Phase (Group) Velocity Observation ...	21
1.5 Regional Variation of Surface Wave Propagation .....	26
Appendix: Formal Definition of Group Velocity .....	32
 <b>Part II. Scattering and Attenuation of Seismic Waves .....</b>	 <b>37</b>
2.1 Coda Waves of Local Earthquakes .....	39
2.2 Fluctuation of Amplitude and Phase Observed by Seismic Arrays .....	58
Appendix A: Derivation of Coda Decay Formulation with the Single Scattering Model .....	66
Appendix B: Averaged Scattered Wavefield as a Function of Autocorrelation of Velocity Fluctuations .....	69
 <b>References .....</b>	 <b>72</b>

## Part I. Surface Waves

The following examples show that surface waves are dominant in many seismograms: from strong motion data ( $\Delta < 8$  km) to global network data ( $\Delta \sim 180^\circ$ ). That is why we can retrieve some important information on the Earth's structure and source processes with surface wave analysis, in addition to other seismic phases such as P and S waves.

- The first synthetic seismogram by Lamb (1904) for a two-dimensional homogeneous half space (Fig.1.1)
- long-period record of global networks such as WWSSN and GDSN (Figs.1.2 and 1.3)
- strong motion data recorded away from faults (Fig.1.4)

Surface waves generally have a large amplitude because body waves (P, S waves) spread out in a medium three-dimensionally while surface waves propagate along the free surface, in other words, two-dimensionally (Fig.1.5), where the amplitude decays

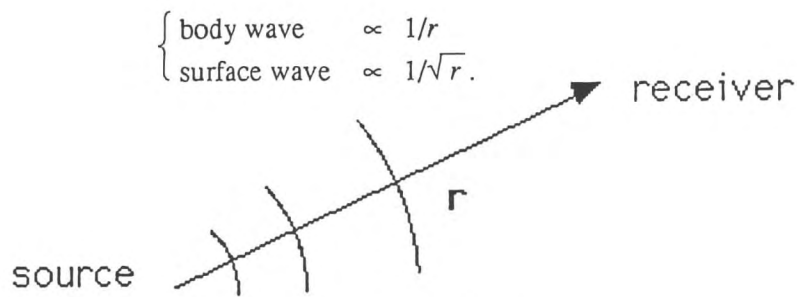


Fig. 1.5: Spatial decay of seismic waves.

Because of the large amplitude and relatively low frequency, it is easy to deal with surface waves in terms of theoretical approaches to waves that were indeed applied for the first time in the history of seismology.

### 1.1 Love and Rayleigh waves

When seismic plane waves interact with a flat free surface in a homogeneous isotropic medium, we can completely separate them into the following two types of waves: SH waves and P-SV waves. When an SH wave is incident to a free surface, only the SH wave is reflected, while both P and SV waves are reflected in the case of either P or SV wave incidence. In other words, P and SV waves are coupled but decoupled from SH waves (Fig.1.6). In a similar sense, we have two types of surface waves (Figs.1.7 and 1.8):

- $$\begin{cases} \text{transverse component (SH type)} & \dots \text{ Love wave} \\ \text{vertical \& radial components (P-SV type)} & \dots \text{ Rayleigh wave} \end{cases}$$

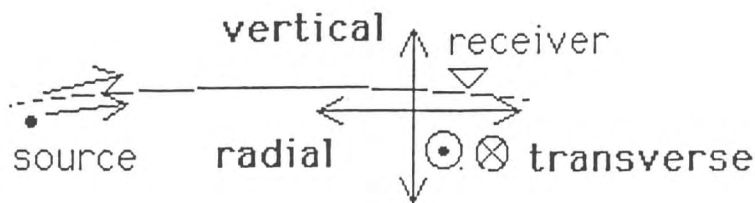


Fig. 1.8: Three components of surface waves.

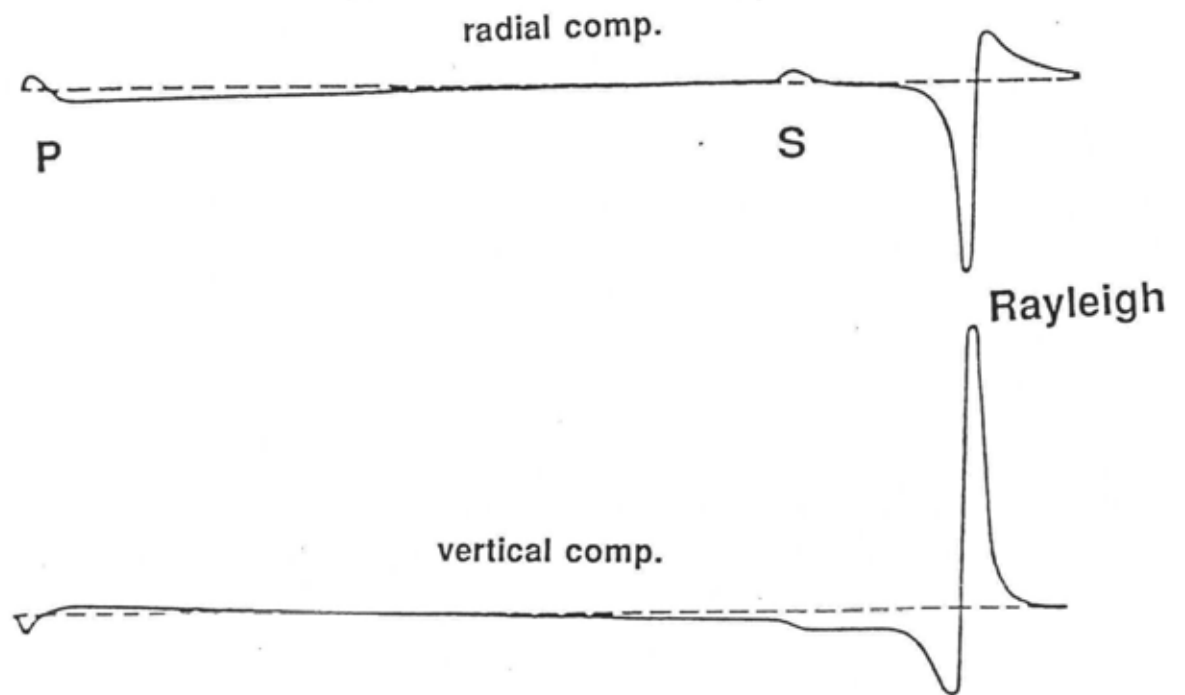


Fig.1.1: The first synthetic seismogram by Lamb (1904) for a point force in a homogeneous half space. From: Lamb, H., On the propagation of tremors over the surface of an elastic solid, Phil. Trans.Roy. Soc. London, A203, 1-42, 1904. (Copyright by Royal Society)

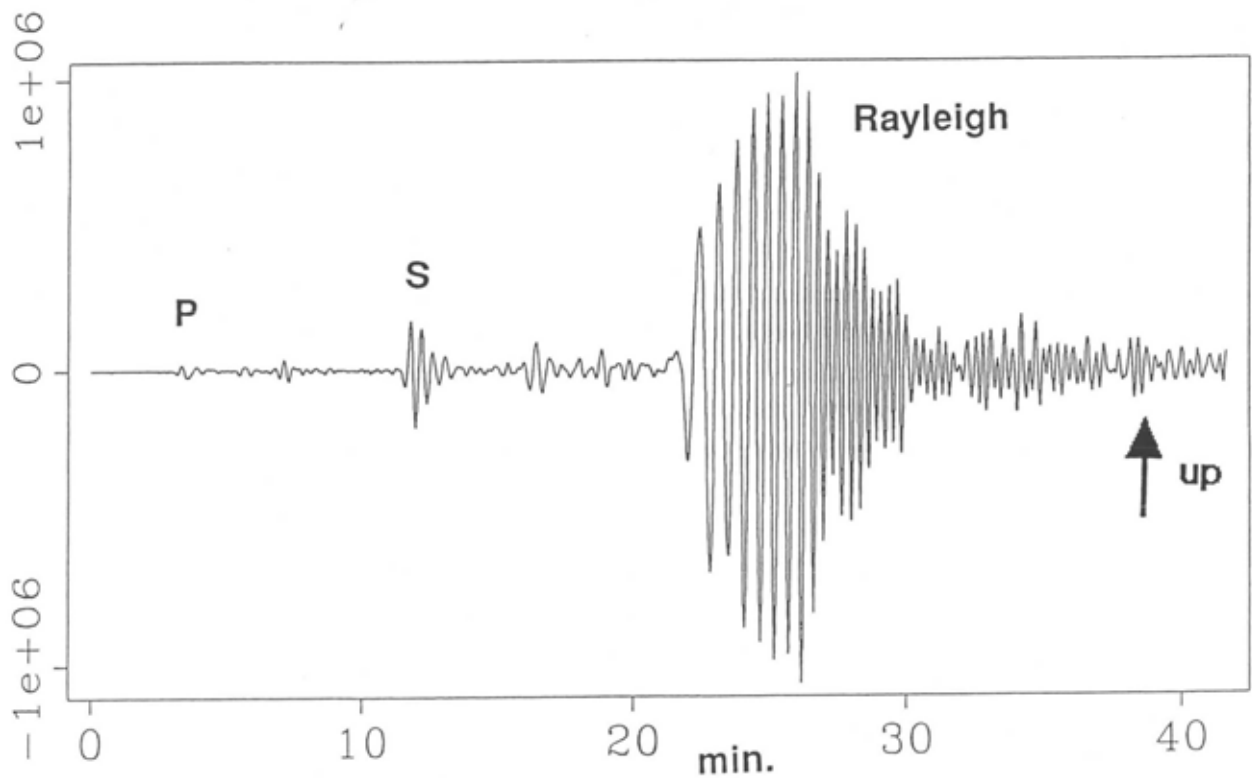


Fig. 1.2: Vertical long-period seismogram recorded at Albuquerque, New Mexico, U.S.A. for an earthquake occurring in the North Atlantic on January 1, 1980.

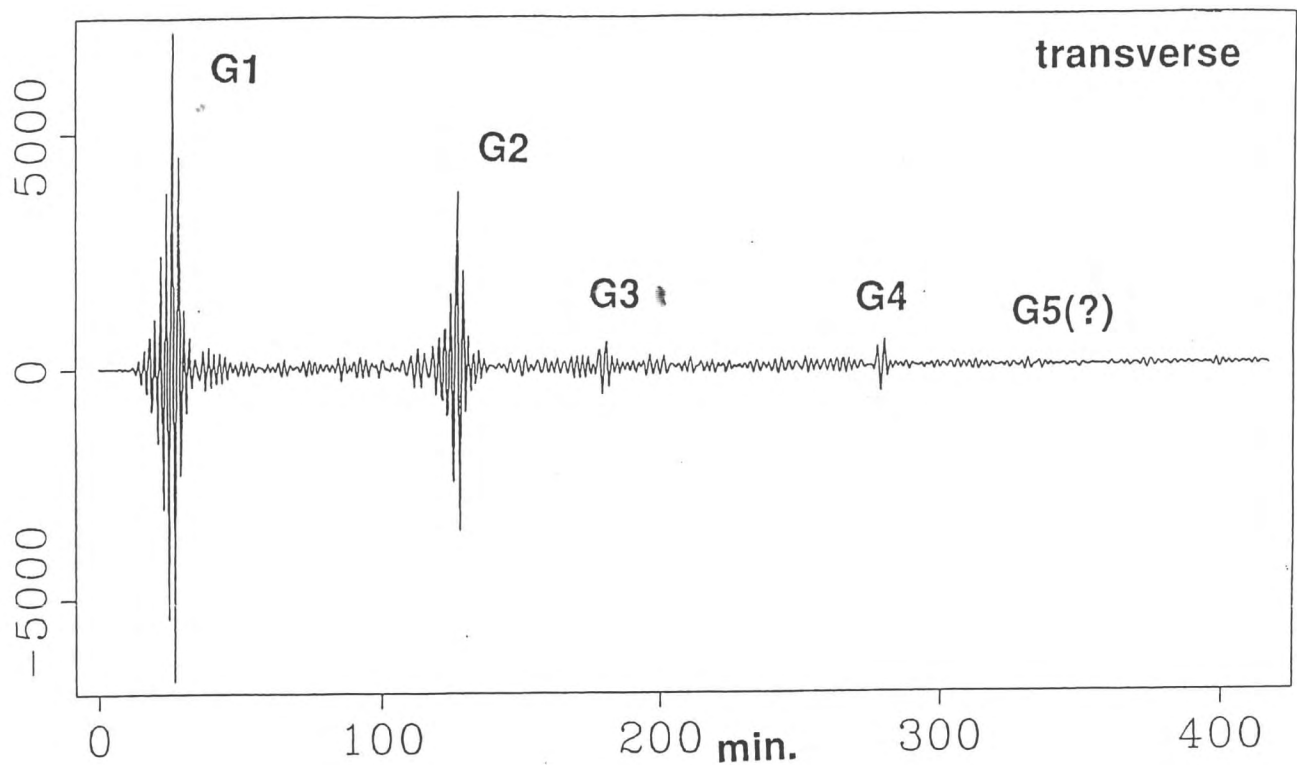


Fig. 1.3: Transverse long-period seismogram for the same station and event as Fig. 1.2. This record is low-pass filtered with the shortest period being 50 sec. Multi-orbit Love waves such as G1, G2 and so on are clearly identified.

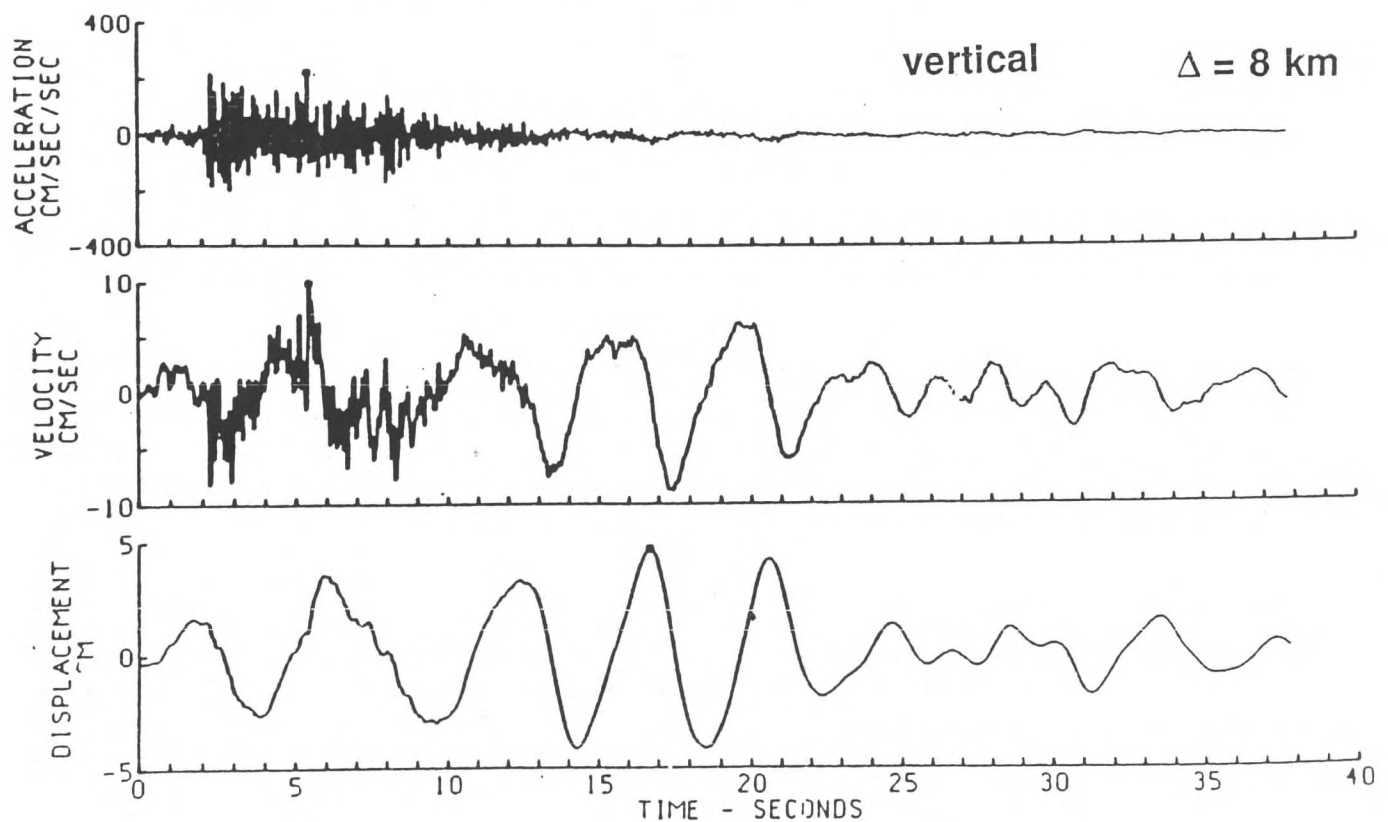


Fig. 1.4: Vertical strong motion seismogram recorded at Holtville Post Office during the Imperial Valley, California, earthquake of October 15, 1979. The distance to the ruptured fault is about 8 km.

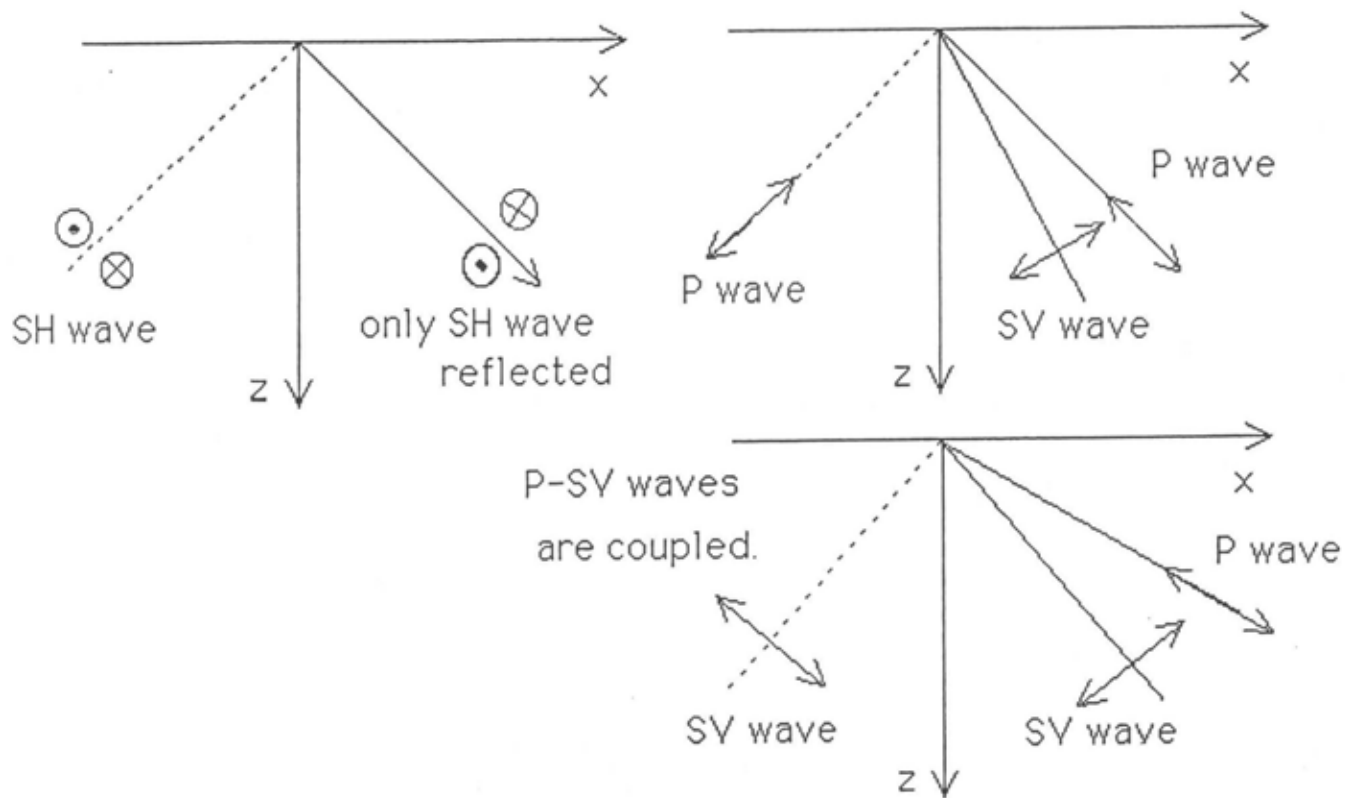


Fig. 1.6: Reflection of seismic waves at a free surface.

This figure is masked  
due to copyright problem.

Fig.1.7: Ground motions of P, S, Love and Rayleigh waves [Bolt, 1976]. (Copywrite by W.H.Freeman and Company)

## 1.2 Dispersion of Surface Waves

Now let's look at how to analyze surface waves in order to study the velocity structure of the earth and source processes. Surface waves have one peculiar character that is distinguished from body waves such as P and S waves (Figs.1.9 and 1.10):

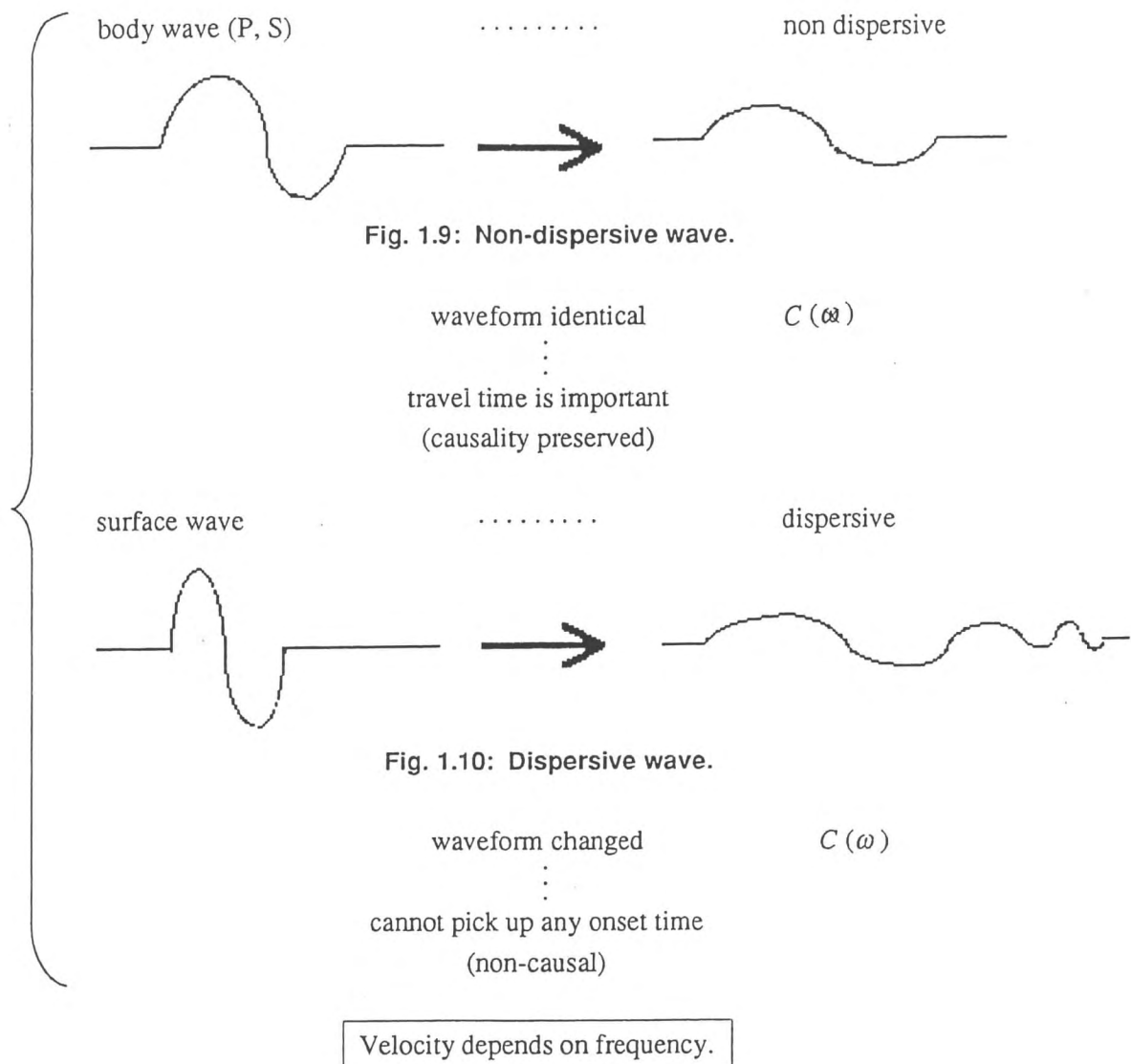


Fig. 1.9: Non-dispersive wave.

Fig. 1.10: Dispersive wave.

First of all, we cannot define travel time of surface waves as we can for body waves. Furthermore, due to the above essential characteristics of surface waves, it is more straightforward to study the frequency domain, instead the waveforms themselves (Fig.1.11):

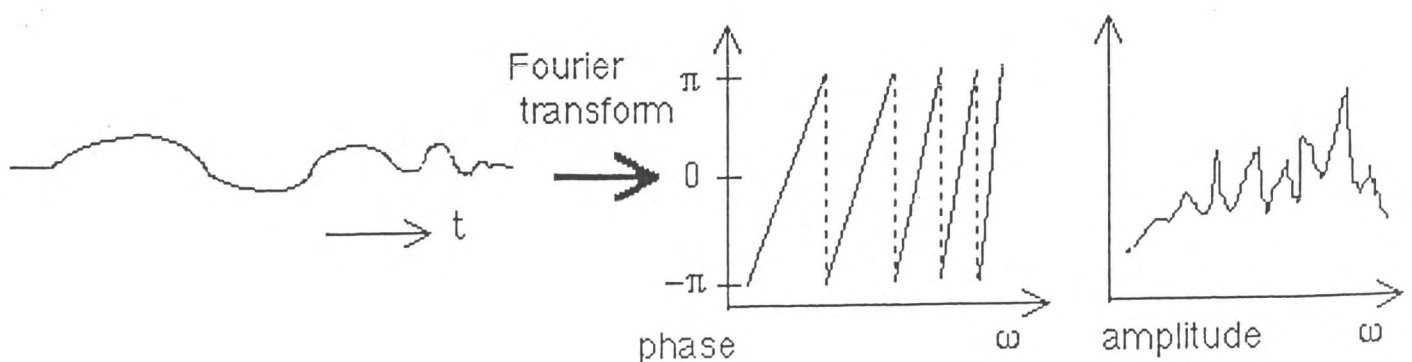


Fig. 1.11: Seismograms in time and frequency domains.

These phase and amplitude spectrals are affected by both propagation (i.e., structure of the earth) and excitation (i.e., source mechanism) processes. In order to understand the basic concept on how to separate these two effects, let us consider an idea called the impulse response. We assume a system with an input named  $s(t)$ . Then, we obtain its output as  $y(t)$ . Next, we are supposed to input the simplest signal: an impulse expressed by the delta function  $\delta(t)$ . The output from the system in this case is denoted by  $x(t)$  as shown in Fig. 1.12.

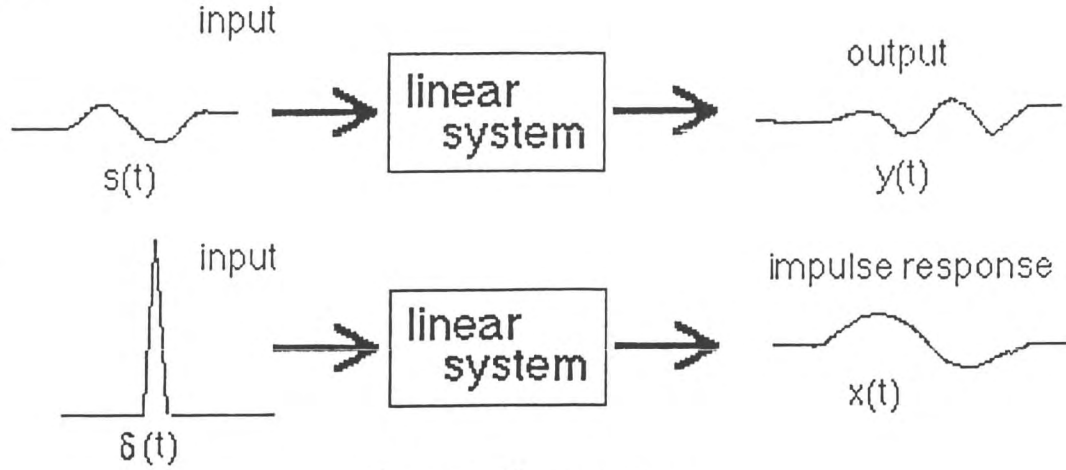


Fig. 1.12: Linear system.

We can easily express the relationship between the input  $s(t)$  and the output  $y(t)$  by following expression:

$$\begin{aligned} y(t) &= x(t) * s(t) \\ &= \int_{-\infty}^{\infty} x(t - \tau) s(\tau) d\tau \end{aligned}$$

where  $*$  is called the convolution. From the convolution theorem (see “Mathematics II” in this lecture series), the above operation corresponds to a simple multiplication in the frequency domain:

$$Y(\omega) = X(\omega) S(\omega)$$

where  $Y(\omega)$ ,  $X(\omega)$  and  $S(\omega)$  are the Fourier transforms of  $y(t)$ ,  $s(t)$  and  $x(t)$ , respectively. Since  $x(t)$  is purely related to any characteristics of the system, we may call it the structural term. Particularly, when its source is an impulse  $\delta(t)$ ,  $x(t)$  or  $X(\omega)$  is called Green's function. Green's function is purely related to the velocity structure  $v(z)$ .  $s(t)$  can be called the source term, and  $y(t)$  is the observation. The above formulation shows that the observation is a simple multiplication of the source term and Green's function (i.e., the structure term) in the frequency domain. This formulation clearly shows how we can separate these two effects. In this note, we shall assume to have obtained the source or  $S(\omega)$  from any other additional information.

In summary, there are three steps in studying velocity structure with surface waves: (1) surface wave seismogram  $y(t)$ , (2) phase velocity  $C(\omega)$  as a function of frequency or dispersion curve explained later, and (3) velocity  $v(z)$  as a function of depth. We shall explain how to measure the dispersion curve from original seismograms in Chapter 1.3, and the relationship between  $C(\omega)$  and  $v(z)$  will be explained briefly in Chapter 1.4. The energy of short-period surface waves is trapped near the surface, while more energy penetrates into deeper parts for long-period surface waves, as schematically shown in Fig. 1.13, which is the essential concept of the relationship between  $C(\omega)$  and  $v(z)$ :



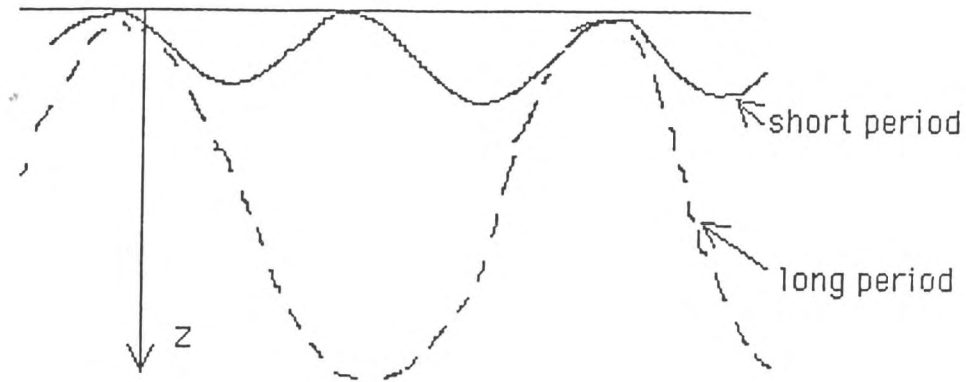


Fig. 1.13: Vertical energy profile of surface waves.

Once velocity depends on frequency, it is essential that two kinds of velocities exist to describe the propagation of such dispersive waves: phase and group velocities. We shall explain each of them.

#### (a) Phase Velocity

Let us consider a harmonic wave with a single frequency  $\omega$ , which means that we take a spectral with  $\omega$  in the frequency domain. In the frequency domain, a plane wave travelling in the  $x$ -direction is written as

$$f(x, t) = A e^{i(kx - \omega t)}$$

where  $A$  is the amplitude and  $k$  is the wavenumber at  $\omega$ . The wavefront of a certain phase plane propagates with a velocity of

$$\omega t - kx = \text{const.}$$

or a constant exponential term in the above formulation. The constant phase wavefront of  $\omega$  therefore propagates with the velocity of

$$C(\omega) \equiv \frac{\Delta x}{\Delta t} = \frac{\omega}{k}$$

which is called the phase velocity. We can image that a trough or peak with a given frequency  $\omega$  in the waveform propagates with this phase velocity  $C(\omega)$  (Fig.1.14).

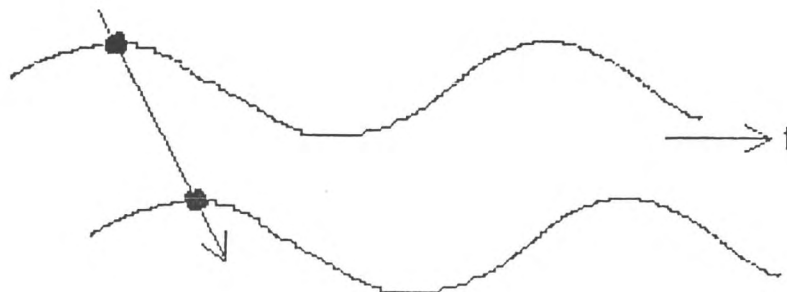


Fig. 1.14: Phase velocity.

## (b) Group Velocity

While the phase velocity is defined in a single frequency or one harmonic sinusoidal wave, an actual surface wave consists of waves with various frequencies. Using a finite frequency band, we view the propagation of one wavepacket while the harmonic waves of each frequency propagate independently at various speeds (i.e., phase velocities). The velocity with which such one wave packet propagates is called the group velocity  $U(\omega)$ . The frequency in this case is defined at the central frequency of the wavepacket. Here we shall define the group velocity by the waves of two adjacent frequencies  $\omega_1$  and  $\omega_2$ . A more general definition of the group velocity is given in Appendix.

Let us consider two harmonic waves with the same amplitude:

$$f_i(x, t) = Ae^{i(k_i x - \omega_i t)} \quad \text{with } \omega_i = c_i k_i, (i = 1, 2).$$

The wavepacket composed of these two waves is then

$$\begin{aligned} f_1 + f_2 &= Ae^{i(k_1 x - \omega_1 t)} + Ae^{i(k_2 x - \omega_2 t)} \\ &= Ae^{i[(k_1 + k_2)x - (\omega_1 + \omega_2)t]/2} \times \{e^{i[(k_1 - k_2)x - (\omega_1 - \omega_2)t]/2} + e^{-i[(k_1 - k_2)x - (\omega_1 - \omega_2)t]/2}\} \end{aligned}$$

Here  $(\omega_1, k_1)$  and  $(\omega_2, k_2)$  are close to each other as defined by

$$\begin{cases} \omega_1 = \omega + \Delta\omega, k_1 = k + \Delta k \\ \omega_2 = \omega - \Delta\omega, k_2 = k - \Delta k \end{cases}$$

Using these variables, we can write the above wavepacket as

$$f_1 + f_2 = 2Ae^{i(kx - \omega t)} \cos(\Delta kx - \Delta\omega t).$$

Since  $k \gg \Delta k$  and  $\omega \gg \Delta\omega$ , the exponential term oscillates much more rapidly than the cosine term. The exponential term can be considered as expressing the phase of the wavepacket in a sense similar to that of a single harmonic wave. In contrast, the cosine term expresses much a slower modulation of its amplitude, which describes the position of the entire wavepacket or the beating of waves with two different frequencies. The cosine term shows how fast the entire wavepacket or the peak-trough of the wave packet propagates. Its velocity can be defined as

$$U(\omega) \equiv \lim_{\Delta k \rightarrow 0} \frac{\Delta\omega}{\Delta k} = \frac{d\omega}{dk}$$

which is called the group velocity. The waves energy propagates with this speed but not the phase velocity. Fig.1.15 summarizes the above concept.

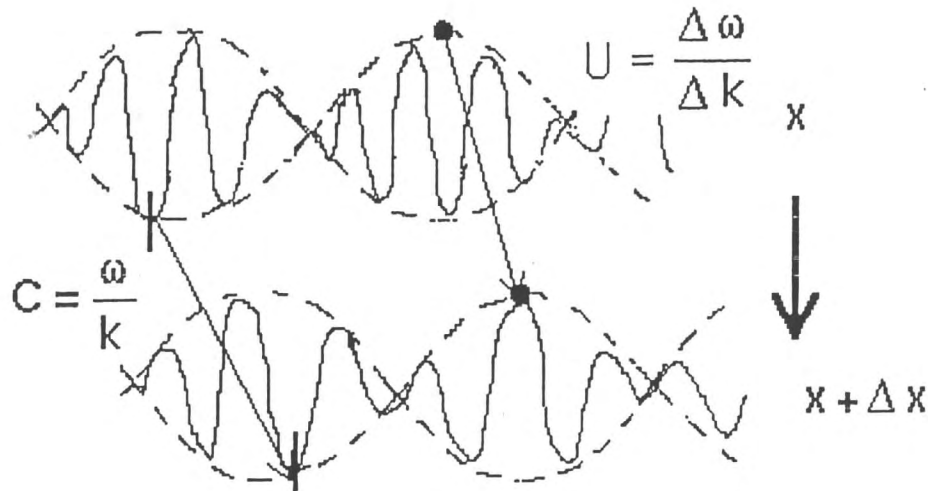


Fig. 1.15: Comparison of phase and group velocities.

In closing this chapter, let us explain one fundamental characteristic of surface waves which distinguishes them from body waves. Waves in general can be expressed by the summation of harmonic waves with each frequency and wavenumber in the form of a double Fourier transform:

$$f(x, t) = \frac{1}{(2\pi)^2} \int_{-\infty}^{\infty} \int_{-\infty}^{\infty} F(\omega, k) e^{i(kx - \omega t)} dk d\omega.$$

In contrast, surface waves can be expressed by a single integration over  $\omega$  because the wavenumber  $k$  cannot be chosen arbitrarily with a given frequency, as expressed in the Appendix:

$$f(x, t) = \frac{1}{2\pi} \int_{-\infty}^{\infty} F(\omega, x) e^{i(k(\omega)x - \omega t)} d\omega$$

with  $k(\omega) = \omega / C(\omega)$ . For surface waves,  $k(\omega)$  or  $C(\omega)$  can exist only with discrete values for a given frequency, which is due to the constraint of boundary conditions. This characteristic, which is called a “mode”, appears when a body is finite.

A simple example of a mode is the vibration of a string fixed at both ends with a force applied at one point, as illustrated in Fig.1.16.

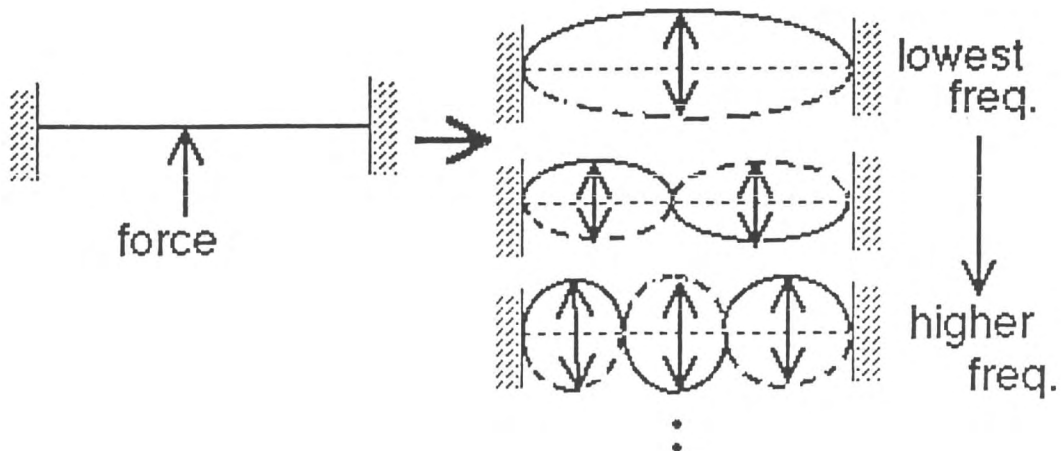


Fig. 1.16: Oscillation of a string fixed at both ends.

The motion of the lowest frequency 'i.e. without nodes' is called the fundamental mode, of a higher frequency with one node is called the first higher mode, with two nodes is called the second higher mode, and so on. In a similar sense, the vertical energy profile classifies the type of surface wave as shown in Fig. 1.17.

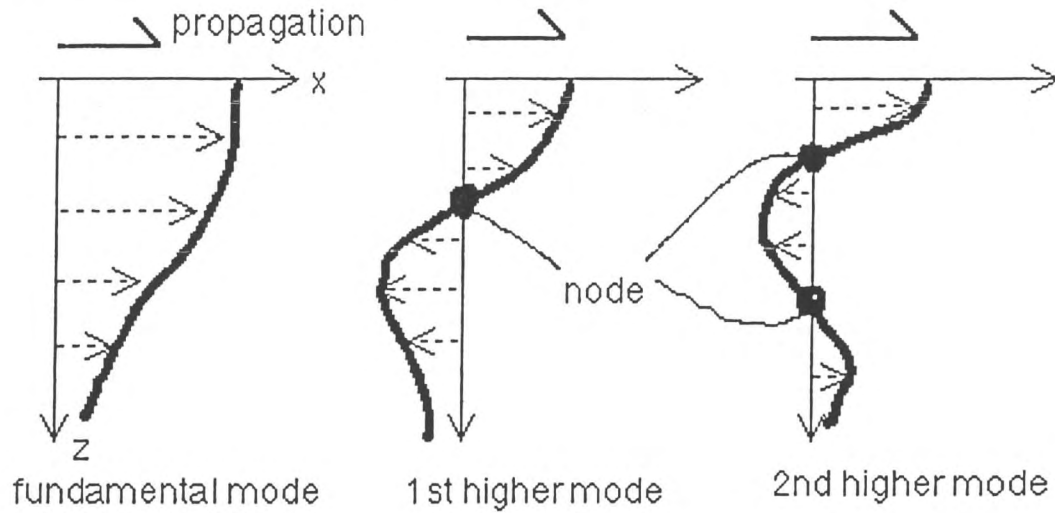


Fig. 1.17: Mode of surface waves.

For the fundamental mode, its amplitude (or energy) decays almost continuously, without nodes, according to depth. The first higher mode has one node at a certain depth with a faster phase velocity for the same frequency. Strictly speaking, we need to consider all kinds of surface waves, but except for deep earthquakes, the fundamental mode is dominant in seismograms, and we assume only this mode to be contained in a seismogram.

### 1.3 Measurement of Phase and Group Velocities

In this chapter, we shall discuss some basic techniques for measuring phase  $C(\omega)$  and group  $U(\omega)$  velocities using actual records.

#### (a) Group Velocity

Since the group velocity is defined by the arrival of a wave packet or its energy, we can measure it by finding the arrival of the maximum amplitude in a given finite but narrow frequency range, once we know its origin time  $T_0$ .

#### 1. Peak-and-trough method

We measure arrival times of peaks and troughs of a surface wave in a record as shown in Fig. 1.18 by  $T_1$ ,  $T_2$ ,  $T_3$  and so on.

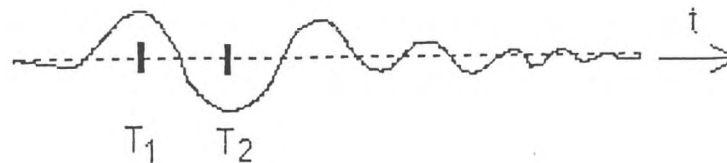


Fig. 1.18: Peak-and-through method for group velocity.

The arrival time of the surface wave around  $\omega_1 = \pi / (T_2 - T_1)$  is then given by

$$T_g \equiv \frac{T_1 + T_2}{2}$$

and the group velocity is obtained simply by the travel distance  $x$  divided by its travel time,  $T_g - T_0$ :

$$U(\omega_1) = \frac{x}{T_g - T_0}.$$

This method is simple and can be easily used for analog records, so it was used in the early stage of surface wave studies during the 1950's and 60's.

## 2. Moving-window analysis

The peak-and-trough method is effective only with beautifully dispersed surface waves. In many cases, it cannot be applied directly because

- Not only a single mode but several modes are usually contained in one seismogram,
- Group velocity does not always increase (or decrease) continuously with frequency,
- There is much noise contamination for various reasons such as multipath propagation due to strong lateral heterogeneities.

Taking advantage of “digital signal processing”, we can measure group arrival time more accurately even for data with much noise. One standard approach is the moving-window analysis explained as follows.

Let us define a seismogram  $f(t)$  and its Hilbert transform  $g(t)$ , which is advanced in phase by  $\pi/2$  (e.g.,  $\cos \omega t \rightarrow \sin \omega t$ ) (Fig.1.19).

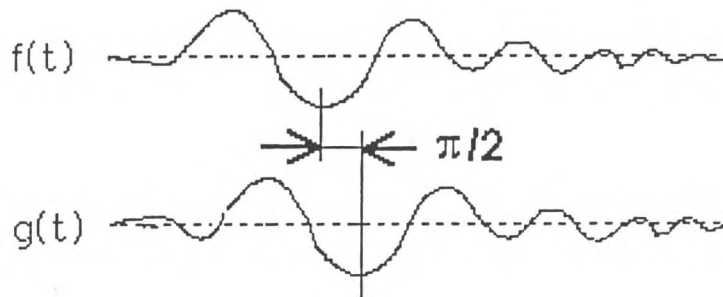


Fig. 1.19: Hilbert transform.

Next we define “instantaneous” amplitude  $A(t)$  and phase  $\Phi(t)$  as

$$A(t) \exp(i \Phi(t)) = f(t) + i g(t),$$

or

$$A(t) = [f(t)^2 + g(t)^2]^{1/2},$$

$$\Phi(t) = \tan^{-1} [g(t)/f(t)],$$

and  $A(t)$  indeed represents the envelope of the wave packet (Fig.1.20).

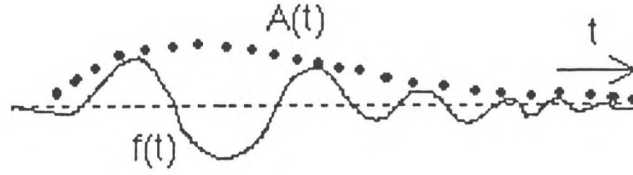


Fig. 1.20: Envelope  $A(t)$  of  $f(t)$ .

Actually, the stationary phase method

$$d\Phi(t)/dt = \omega(t)$$

leads to the peak-and-trough method described above. Similarly, the maximum amplitude for a narrow frequency band seismogram with the central frequency  $\omega_n$  (band-pass filtered) gives a group travel time to obtain the group velocity (Fig.1.21):

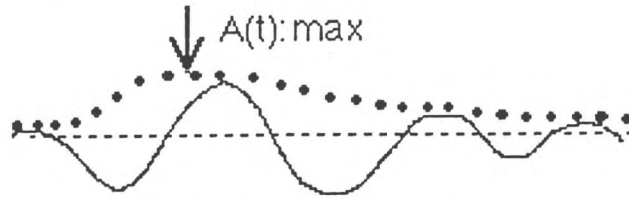


Fig. 1.21: Group arrival.

The Gaussian filter is one of the simplest band-pass filters used (Fig.1.22):

$$H(\omega, \omega_n) = \exp \left[ -\alpha \left( \frac{\omega - \omega_n}{\omega_n} \right)^2 \right]$$

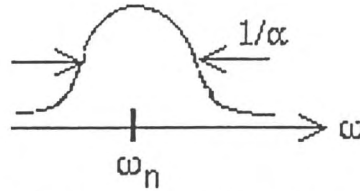


Fig. 1.22: Gaussian filter.

where  $\alpha$  measures its bandwidth. More conventional is the use of the truncated Gaussian filter (Fig.1.23):

$$H(\omega, \omega_n) = \begin{cases} 0 & \omega < (1-\beta)\omega_n \\ \exp \left[ -\alpha \left( \frac{\omega - \omega_n}{\omega_n} \right)^2 \right] & (1-\beta)\omega_n \leq \omega \leq (1+\beta)\omega_n \\ 0 & (1+\beta)\omega_n < \omega \end{cases}$$

where  $\beta$  represents the non-zero frequency width of the filter.

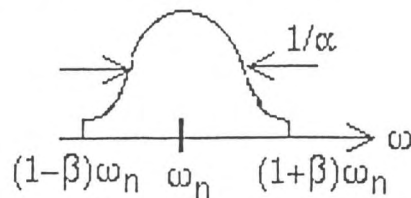


Fig. 1.23: Truncated Gaussian filter.

By experience,  $\beta \sim 0.25$  is appropriate for most seismograms.

Let us summarize the moving-window analysis:

1. seismogram  $f(t)$

Using the Fourier transform, we get

$$F(\omega) = \int_{-\infty}^{\infty} f(t) e^{i\omega t} dt.$$

2. Selection of an appropriate bandpass filter with a certain central frequency  $\omega_n$ . Then we get the windowed spectral for  $\omega_n$

$$F_n(\omega) = H(\omega, \omega_n) F(\omega).$$

3. Hilbert transform of  $F_n(\omega)$  denoted by  $Q_n(\omega)$ :

$$\text{Re}\{Q_n(\omega)\} = -\text{Im}\{F_n(\omega)\},$$

$$\text{Im}\{Q_n(\omega)\} = \text{Re}\{F_n(\omega)\},$$

which means that there is  $\pi/2$  phase difference between  $F_n(\omega)$  and  $Q_n(\omega)$ .

4. Inverse Fourier transforms of  $F_n(\omega)$  and  $Q_n(\omega)$ :

$$f_n(t) = \frac{1}{2\pi} \int_{-\infty}^{\infty} F_n(\omega) e^{-i\omega t} d\omega,$$

$$q_n(t) = \frac{1}{2\pi} \int_{-\infty}^{\infty} Q_n(\omega) e^{-i\omega t} d\omega.$$

5. Computation of instantaneous amplitude (i.e., envelope) with  $f_n(t)$  and  $q_n(t)$  (Fig.1.24):

$$A_n(t) = [f_n(t)^2 + q_n(t)^2]^{1/2}$$

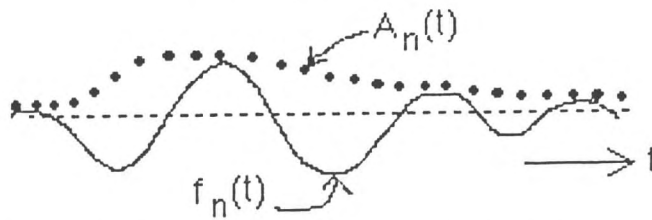


Fig. 1.24: Bandpass filtered seismogram  $f_n(t)$  and its envelope  $A_n(t)$ .

6. Pick up group arrivals:

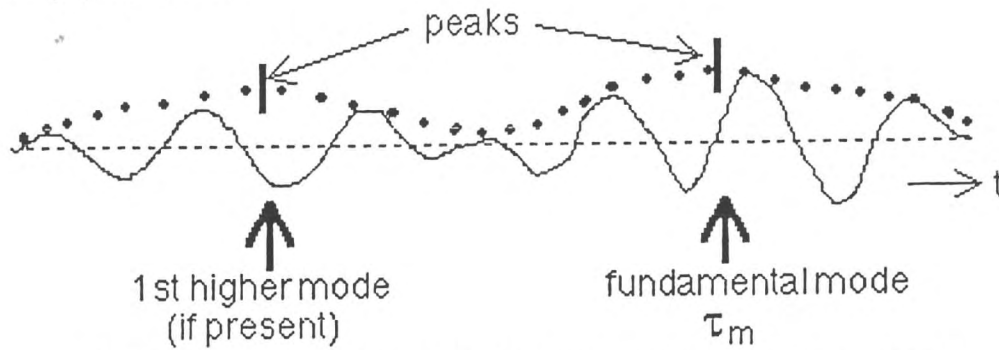


Fig. 1.25: Bandpass filtered surface wave record with several modes.

with peaks of the envelope, denoting  $\tau_m$  (Fig.1.25).

7. Group velocity at  $\omega_n$  is then given by

$$U(\omega_n) = \frac{x}{\tau_m - \tau_0}$$

where  $x$  is the epicentral distance and  $\tau_0$  is the origin time.

One usually displays seismograms  $f_n(t)$  or their instantaneous amplitudes  $A_n(t)$  as a function of  $U(\omega_n)$  computed from known values of  $x$  and  $\tau_0$  instead of the time itself, as shown in Fig. 1.26.

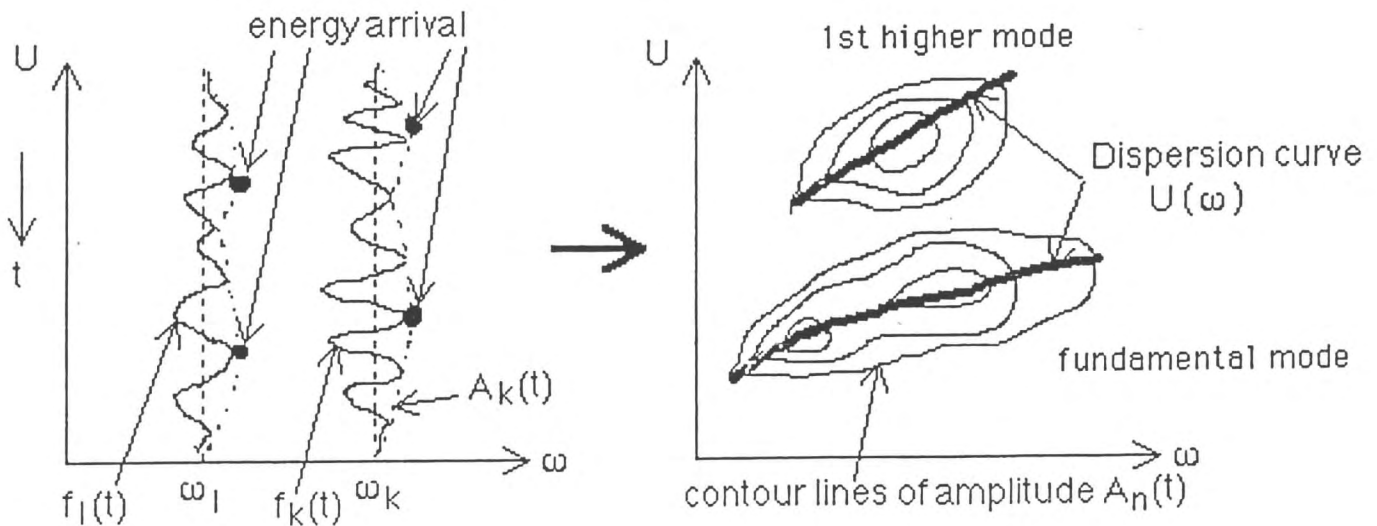


Fig. 1.26: Moving-window analysis for group velocity.

Several peaks in  $A_n(t)$  for larger values of  $U(\omega_n)$  may represent the group velocities of higher modes in this analysis. The key point in using this analysis effectively is the optimal choice of the width of the moving window,  $\alpha$ , so as to obtain good resolution. If  $\alpha$  is too small or the frequency bandwidth is large, we get poor resolution in frequency while the resolution in velocity is poor with a large value of  $\alpha$ . Many numerical examples and computations with actual seismograms show the appropriate bandwidth to be 4-th ~ 12-th of the considered frequency  $\omega_n$ . The following examples (Fig.1.27-29) are taken from Dziewonski and Hales (1972) to show how this analysis works.



# FREQUENCY AND TIME DOMAIN FILTERING

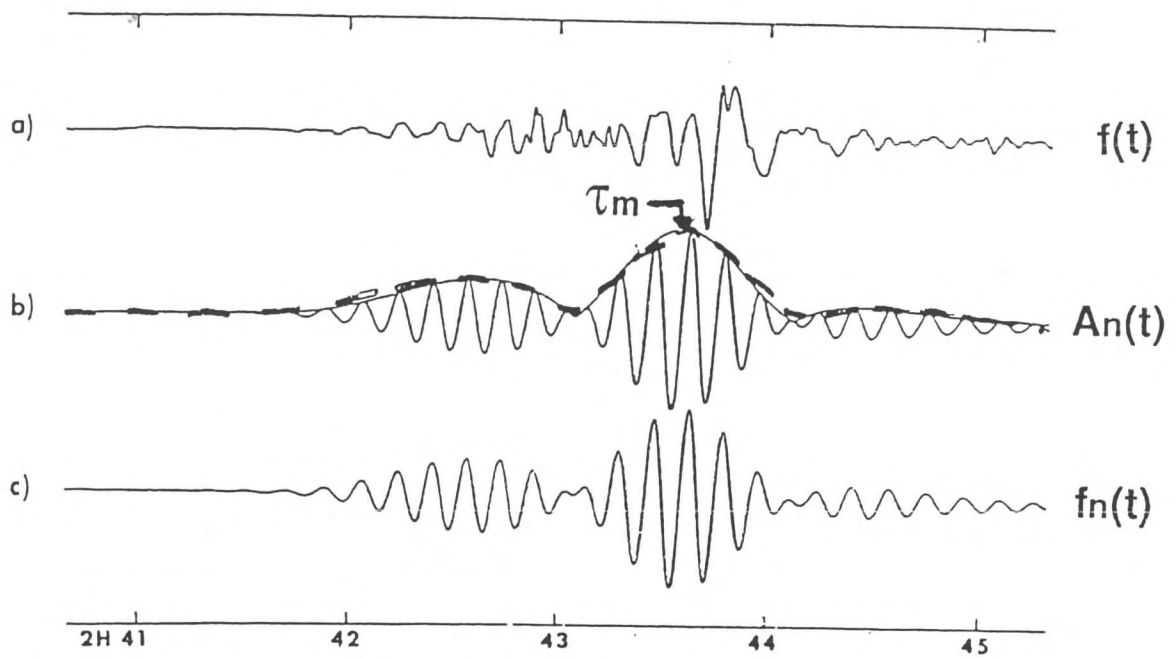


Fig. 1.27: Original seismogram  $f(t)$ , bandpass filtered seismogram  $f_n(t)$  and its envelope  $A_n(t)$  with group arrival  $\tau_m$  [after Dziewonski et al., 1969].

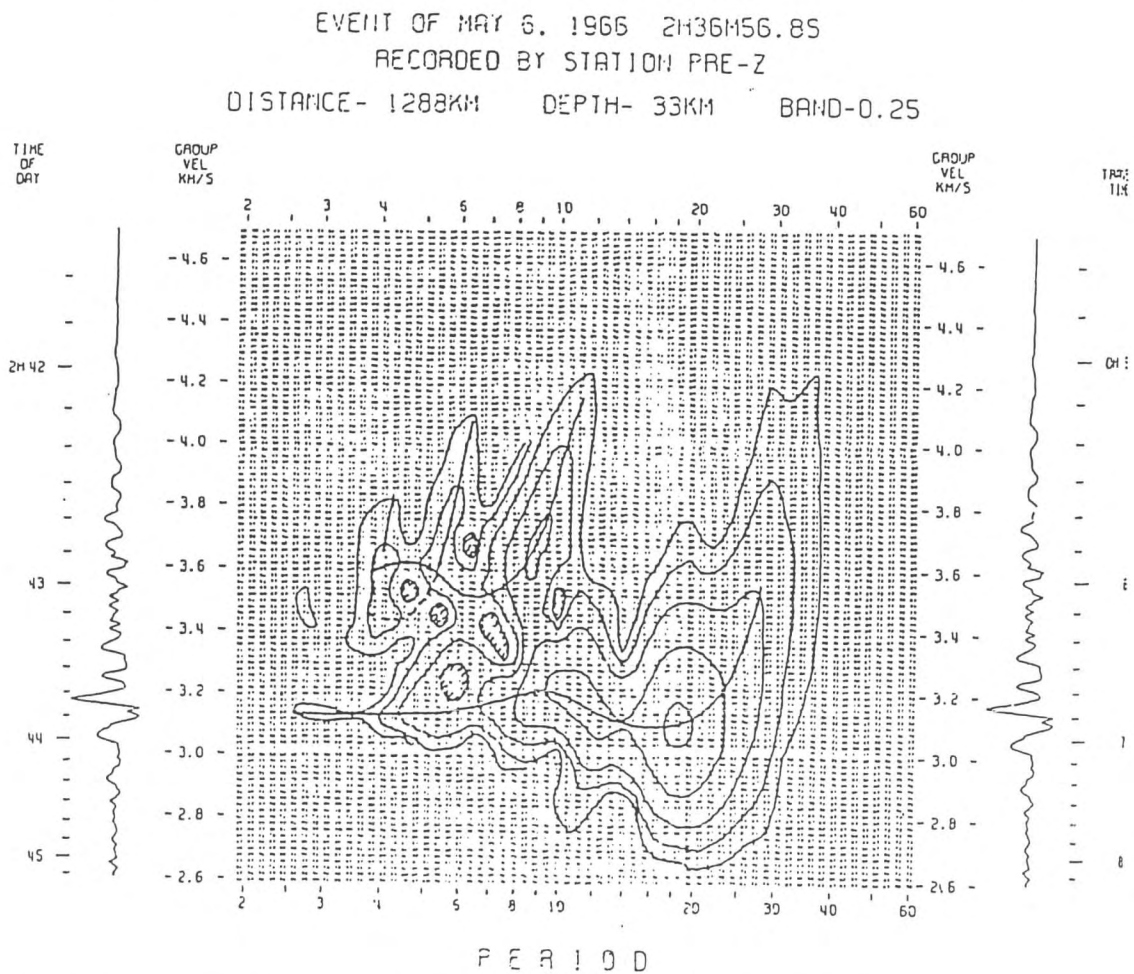


Fig. 1.28: Moving window analysis of surface wave seismogram with several modes [Bloch et al. 1969].



This figure is masked  
due to copyright problem.

Fig.1.29: Example of moving window analysis and filtered seismogram using the obtained dispersion curve of group velocity [Dziewonski and Hales, 1972].

### (b) Phase velocity

Unlike group velocity, we need additional information to measure phase velocity. We shall explain how to obtain or rather “skip” such extraneous information. First of all, in the present discussion, we assume that waveforms consist simply of one mode without any other contaminating modes. This assumption can be verified with the following procedures in actual cases.

- For shallow events, the fundamental mode is dominantly excited.
- “Group velocity windowing”: Filtering out some portions of the seismogram outside the range of expected arrival of a given mode estimated from any standard group velocity model
- Filtering out undesired modes by the moving window analysis first, which is explained above.
- Polarization (vertical vs radial components) of Rayleigh waves is different for each mode, so we can pick up one specific mode by plotting polarizations of seismogram.
- Stacking (not explained here)

Most of the above procedures to select a desired mode use some kind of “filtering”, but we must take some caution in using such filters because filtering often causes distortion of the original phase information or alters its waveform.

A seismogram for surface wave with one mode can be expressed by

$$f(x, t) = \frac{1}{2\pi} \int_{-\infty}^{\infty} |G(\omega)| e^{-i\omega \left( t - \frac{x}{C(\omega)} \right) + i\phi(\omega)} d\omega$$

which can be directly compared with the simple Fourier transform of the original seismogram  $f(x, t)$ :

$$F(\omega) = \int_{-\infty}^{\infty} f(x, t) e^{i\omega t} dt.$$

$\phi(\omega)$  is the phase term related to any factors other than the propagation effect between a source and a receiver. Comparing these two equations, the phase of the seismogram,  $\Phi(x, \omega)$ , is related to the exponential term in the former equation as

$$\Phi(x, \omega) \equiv \tan^{-1} \left( \frac{\text{Im } F(\omega)}{\text{Re } F(\omega)} \right) = -\omega t_0 + \frac{x\omega}{C(\omega)} + \phi(\omega) + 2n\pi$$

where  $n$  is any interger and  $t_0$  is the initial time of a given seismogram with respect to its origin time. The above term  $2n\pi$  appears due to the periodicity of the imaginary exponential function.

Since  $\Phi(x, \omega)$  is obtained from observed data and we presume the existence of  $x$  and  $t_0$ , the following two values must be estimated to obtain the phase velocity value  $C(\omega)$ :

1.  $\phi(\omega)$  a priori
2.  $2n\pi$  ambiguity

The latter ambiguity of  $n$  cannot be removed rigorously but we can get a fairly good approximation of it from any selected initial velocity model if it is not far from the observation. Particularly in the low frequency range, an erroneous choice of  $n$  would yield anomalous phase velocity values. We thus obtain quite reliable estimates of  $n$ . The estimation of  $\phi(\omega)$  is therefore the final obstacle to obtaining phase velocity values.  $\phi(\omega)$  is the phase delay related to instrumental response and the source, which is determined by source processes such as focal mechanisms. There are several approaches to estimating the value of  $\phi(\omega)$ .

### 1. Two-station method

Suppose that we have two stations located on the great circle connected to the source, and  $\Phi_1(\omega)$  and  $\Phi_2(\omega)$  are the observed phases at these stations (Fig.1.30). By comparing the two phases and remembering the previous expression for the phase term, we get

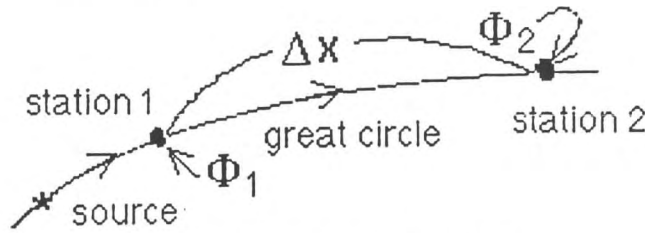


Fig. 1.30: Two-station method.

$$\Phi_2(\omega) - \Phi_1(\omega) = \frac{\omega \Delta x}{C(\omega)} + 2l\pi$$

where  $\Delta x$  is the distance between the two stations and  $l$  is an arbitrary integer. Since both stations record the wave radiated in the same direction at the source, the term  $\phi(\omega)$  is common and we can eliminate it by comparing these two observed phases. By estimating the arbitrary integer  $l$  in some way, we obtain the value of phase velocity  $C(\omega)$ . If we have more observations along the great circle, we can even estimate  $l$  individually. This has been done in several studies using such as the tripartite method (three stations) by F. Press and the multi-station method (more than three) by K. Aki around 1960.

This approach, however, has the following major difficulties:

- It is rare to find two stations along one great circle connected to the source.
- It is greatly affected by any laterally reflected waves if the stations used are not exactly on the great circle.

### 2. Multi-orbit method

For large earthquakes ( $M > 5.5$  in the present global networks) we obtain multi-orbit surface waves as schematically shown in Fig. 1.31 and an example of which was given earlier in Fig. 1.3. These waves propagate along the great circle many times around the Earth (Fig.1.32).

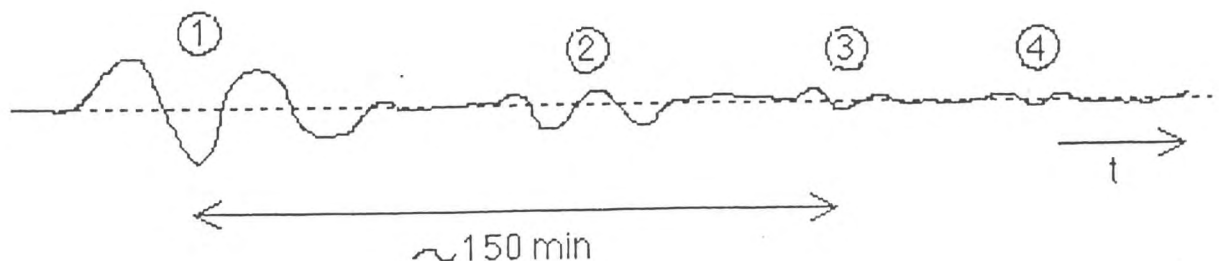


Fig. 1.31: Multi-orbit surface waves.

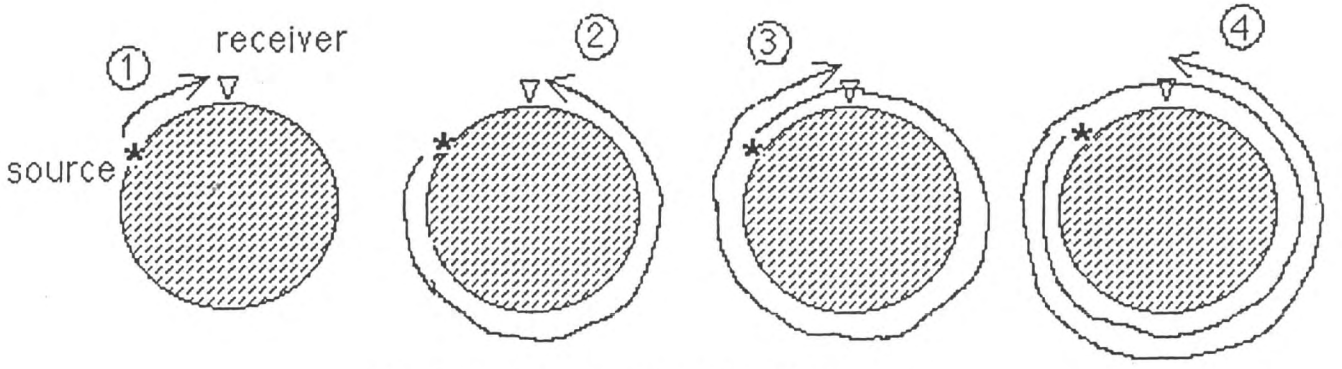


Fig. 1.32: Path of multi-orbit surface waves.

For odd-order orbits (denoted #1, #3, and so on in Fig. 1.32), the direction of radiated waves from the source is common, which means they share the same value of  $\phi(\omega)$ . The same goes for even-order orbits (e.g., #2, #4, and so on). If we take the phase spectrals  $\Phi_i(\omega)$  of a part of the seismogram corresponding to the  $i$ -th orbit surface wave and compare two of the same type (odd or even), we can eliminate the term  $\phi(\omega)$  by

$$\Phi_{i+2}(\omega) - \Phi_i(\omega) = \frac{\omega L}{C(\omega)} + 2l\pi - \pi$$

where  $L$  is the great circle length on the Earth and  $l$  is an arbitrary integer as discussed above. The last term  $\pi$  in the right hand side is related to the “polar phase shift”. When surface waves reach either the pole (i.e., source location) or the antipode (i.e., the opposite point to the pole on the earth sphere), all the radiated energy converges and then goes outwards. This phenomenon is similar to the focusing effect in the study of the travel times of P or S waves. In such a case, the phase of any wave is advanced by  $\pi/2$ . Since the  $(i+2)$ -th orbit wave passes through both of the pole and the antipode once more compared to the  $i$ -th orbit (Fig. 1.33). We therefore need to correct the additional phase shift by  $\pi$ .

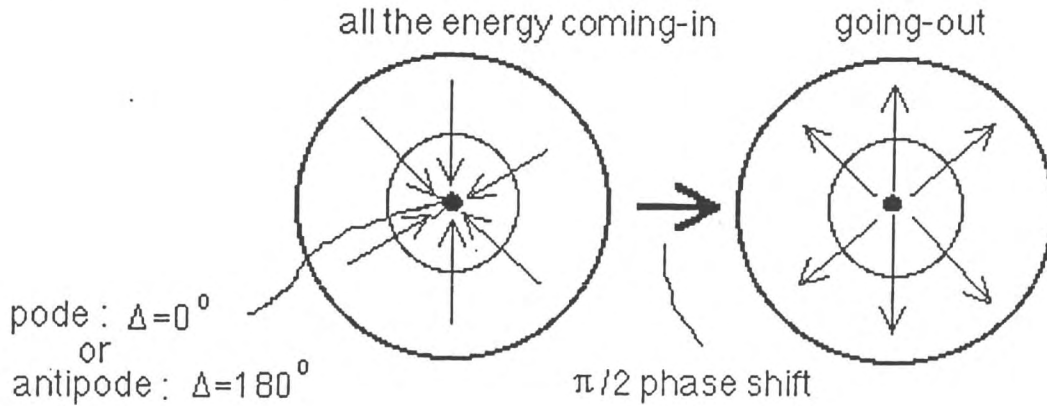


Fig. 1.33: Polar phase shift at pole or anti-pole.

With the above formulation, we can estimate  $C(\omega)$  along the great circle with one seismogram. This method is particularly used for global variations in phase velocity.

### 3. Single station method

The phase spectral of the seismogram recorded at a station with an epicentral distance of  $x$  is expressed by

$$\Phi(x, \omega) = -\omega t_0 + \frac{\omega x}{C(\omega)} + \phi(\omega) + 2n\pi$$

where  $n$  is the integer to be chosen (Fig. 1.34). Using observations from just one station, we need to estimate  $\phi(\omega)$  to get the phase velocity value  $C(\omega)$ . The single station method uses the above formulation directly with any additional information on  $\phi(\omega)$ .

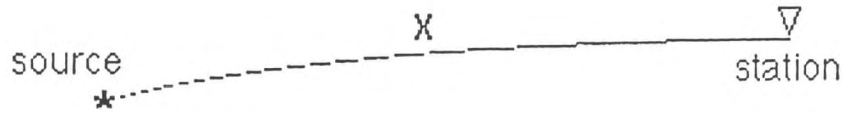


Fig. 1.34: Single station method.

This term can be expressed by three separate terms:

$$\phi(\omega) = \phi_s(\omega) + \phi_f(\omega) + \phi_r(\omega)$$

where

$\phi_s(\omega)$  : initial phase at source depending on its focal mechanism

$\phi_f(\omega)$  : phase delay due to the finiteness of fault area

$\phi_r(\omega)$  : instrument response such as seismometer and recorder.

The third one is probably known with a given record, and we therefore need to estimate the source process relatively well for the first two terms as follows:

1.  $\phi_s(\omega)$

Let us consider a simple example for the P wave initial phase with a pure strike slip earthquake as illustrated in Fig. 1.35.

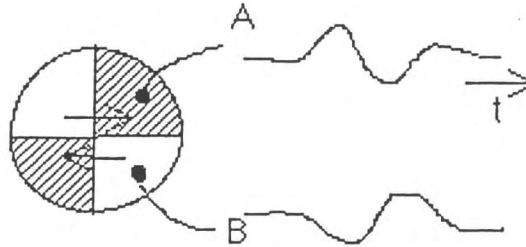


Fig. 1.35: Initial phase depending on focus mechanism.

Two stations separated by an azimuth of  $90^\circ$  apparently display phase difference by  $\pi$  in  $\phi_s$ . Similarly, the initial phase of surface waves is determined by both the focal mechanism and the azimuth of a given observation point. In the case of surface waves, it also depends on the focal depth and velocity structure at the source. Details are given in many textbooks such as Chapter 7 of Aki and Richards (1980). Such information on focal mechanisms is obtained by various methods such as the first motion analysis of a P wave through use of a focal sphere.

2.  $\phi_f(\omega)$

General formulation of this term is very complex, and here we give only one simple example: the Haskell fault model with a unidirectional and unilateral rupture as shown in Fig. 1.36.